Proceedings of IMECE'03
2003 ASME International Mechanical Engineering Congress
Washington, D.C., November 15–21, 2003

IMECE2003-42548

DYNAMIC MODELING OF A HYBRID ELECTRIC DRIVETRAIN FOR FUEL ECONOMY, PERFORMANCE AND DRIVEABILITY EVALUATIONS

Xi Wei, Pierluigi Pisu, Giorgio Rizzoni and Stephen Yurkovich

Center for Automotive Research and Intelligent Transportation
The Ohio State University
930 Kinnear Road
Columbus, Ohio 43212, U.S.A.

ABSTRACT

Both automakers and customers keep on pursuing better fuel economy, performance and driveability. A "mild" hybrid drivetrain is of great interest due to its potential capability on improving these targets. This drivetrain contains a spark ignition (SI) engine, an integrated starter/alternator (ISA), a torque converter (TC), a continuously variable transmission (CVT), a final drive (FD), a driveshaft, a brake-by-wire (BBW) system and wheels. While the challenge is to model and to develop an optimal control algorithm for this hybrid electric vehicle (HEV), this paper will focus only on the modeling aspect. Model-based control design and the nature of human perceptible driveability issues require low-frequency dynamic models. Therefore, a nonlinear control-oriented model which is sufficiently accurate but not excessively complicated is proposed here. Simulation results demonstrate that this model is effective to capture the main behaviors of vehicle dynamics and to evaluate fuel economy, performance and driveability objectively.

NOMENCLATURE

M	vehicle mass in *kg*
RMS	acceleration root mean square value in m/s^2
SOC	battery state of charge
V	vehicle velocity in *m/s*
VDV	vibration dose value in $m/s^{1.75}$
g	gravity acceleration in m/s^2
$grade$	road grade
$idle$	engine idle speed in *rad/s*
$redline$	engine redline speed in *rad/s*
η	lumped ISA, power electronics and battery efficiency
A_f	vehicle frontal area in m^2
B_{eng}	engine damping coefficient
C_d	drag coefficient
C_r	rolling resistance coefficient
D_1, D_2	coefficients of driveshaft nonlinear damper
F_a	aerodynamic force in *N*
F_{brk}	brake force in *N*
F_g	gravity force in *N*
F_r	rolling resistance force in *N*
F_{tr}	total traction force in *N*
J_1	lumped inertia of engine, ISA and TC pump in $N.m.s^2/rad$
J_2	lumped inertia of TC turbine and CVT primary
J_3	lumped inertia of CVT secondary pulley, final drive and wheels in $N.m.s^2/rad$
K_{ds}	lumped driveshaft compliance in *N.m/rad*
$Ksoc$	battery energy capacitance in *J*
$M_1 \sim M_4$	cylinder air mass flow rate coefficients
P_m	intake manifold pressure in P_a
$P_{discharging}$	battery discharging power of in *kw*
$P_{recharging}$	battery recharging power of in *kw*
R_m	ideal gas constant for air
R_{wh}	wheel radius in *m*
T_{brk}	brake torque in *N.m*
T_{clutch_max}	maximum torque converter clutch torque in *N.m*
$T_{cvt\_p/s}$	CVT primary/secondary pulley torque in *N.m*
T_{ds}	driveshaft torque in *N.m*
T_e	engine torque in *N.m*
T_{fd}	final drive torque in *N.m*
T_{isa}	ISA torque in *N.m*
T_{isa_req}	ISA torque request in *N.m*
T_m	atmospheric temperature in *k*
$T_{p/t}$	TC pump/turbine toque in *N.m*
T_{wh}	wheel torque in *N.m*
$T_0 \sim T_6$	engine torque production coefficients
V_m	intake manifold volume in m^3
$a_1 \sim d_3$	TC pump/turbine torque coefficients
r_{cvt}	CVT ratio
r_{fd}	final drive ratio
t_d	engine torque production delay in *s*

η_{cvt}	CVT efficiency
η_{fd}	final drive efficiency
ρ_{air}	air density in kg/m^3
τ_{brk}	BBW time constant in *s*
τ_{cvt}	CVT time constant in *s*
τ_{etb}	ETB time constant in *s*
τ_{isa}	ISA time constant in *s*
$\omega_{cvt\_p/s}$	CVT primary/secondary pulley speed in *rad/s*
ω_{ds}	driveshaft speed in *rad/s*
ω_e	engine speed in *rad/s*
ω_{fd}	final drive speed in *rad/s*
ω_{isa}	ISA speed in *rad/s*
$\omega_{p/t}$	TC pump/turbine speed in *rad/s*
ω_{wh}	wheel speed in *rad/s*
$\dot{m}_{cyl}$	engine air mass flow rate entering the cylinders in *Kg/s*
$\dot{m}_{th}$	air mass flow rate entering the ETB in *Kg/s*
$\dot{m}_{th\_req}$	ETB air mass flow rate request in *Kg/s*

1. INTRODUCTION

Automotive manufacturers have been striving for decades to produce vehicles which satisfy customers' requirements at minimum cost. Many of their concerns are on fuel economy, road performance and driveability. Improving fuel economy is both a political concern of alleviating dependency on foreign fuel and a customer preference of reducing vehicle operating cost. Consumers also expect vehicles to provide satisfactory performance with desirable driving comfort. Improvements on all of the above aspects may contribute to lower emissions as well if the vehicle is designed and controlled properly.

The introduction of innovations and new technologies has never been stopped in vehicle design and control since the first engine-powered car appeared in 1886 [1]. Among these, hybridization with appropriate control is a feasible solution which helps to improve fuel mileage, performance, driveability and emissions simultaneously. Growing demand for auxiliary electric-powered devices, such as electric power steering, active suspension, electric brakes, catalyst heaters, etc., tends to double or triple the current vehicle electric load [2]. An integrated starter/alternator (ISA) with $42V$ system is able to meet this requirement at low cost and is becoming popular around the world. A propulsion system with an ISA coupled to an engine directly or by a belt is referred to as a "mild" or "soft" hybrid.

The continuously variable transmission (CVT) is another attractive technology and became practical after its price was significantly decreased. A CVT is effective to achieve continuously smooth shifting and enables the engine to operate in its most efficient region. The side effect is that it decreases available torque reserve and may have undesirable impacts on driveability before the engine is recalibrated [3]. Frijlink and Schaerlaeckens suggested that if we combine an ISA with a CVT, the ISA can compensate for this deterioration with torque boost capability [3]. Therefore, thorough investigations on a "mild" hybrid powertrain, which consists of a spark ignition (SI) internal combustion engine (ICE), an ISA, a torque converter (TC), a CVT, a final drive (FD), a driveshaft, a brake-by-wire (BBW) system and wheels, (as it is sketched in Fig. 1), is of great interest. The vehicle is proposed to be a front-wheel drive mid to full size passenger sedan. The challenge here is to model and to develop a control algorithm for this hybrid electric vehicle (HEV) to achieve optimal fuel economy, performance and driveability.

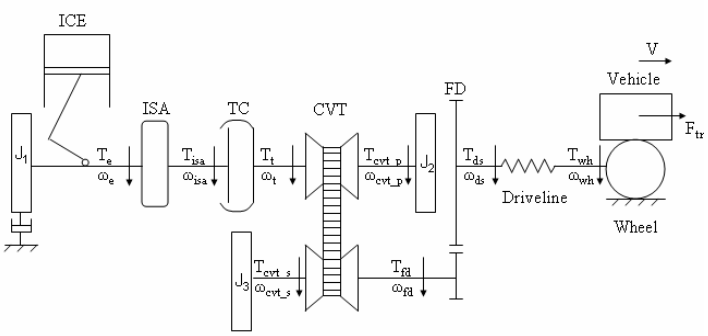

Figure 1. Schematic of a "mild" HEV powertrain

Model-based control design is widely used by control engineers in many fields and obviously it requires a control-oriented model. A system model is classified as static/quasi-static, low-frequency dynamic and high-frequency dynamic based on time scale. The resources of these models can be from experimental data, empirical equations or first principle derivations. Individual cylinder engine model [4-5], five-state electric machine model [6], Hrovat and Tobler's TC model [7] and detailed CVT model [8] are all categorized as the high-frequency dynamic model. These models are of high-order and they are excessively complicated for standard control design [9]. However, control engineers can always design a controller based on a simplified low-frequency, low-order dynamic model, as shown in the literatures [8, 10-14], and then test this control strategy with the high-frequency model if hardware validation is not available.

The "best" model is the one that represents all the phenomena a real system exhibits with the lowest complexity and expense. Due to the existence of model uncertainty and disturbance, none of the models are perfect. However, if a model captures the main behaviors of a physical system with satisfactory accuracy, we consider that it is acceptable and valid. Obviously, a model can only be evaluated after its application has been determined. A quasi-static model is adequate for fuel economy and performance study [15], but it is definitely not sufficient for evaluating driveability issues. Dynamics of driveability are in the frequency of a few *hertz* in a real vehicle, thus we need a low-frequency dynamic model. Both the system model and its control algorithm need to be tested in simulation before one builds a prototype.

In contrast to a "backward" simulator which accomplishes computations backwards based on known vehicle velocity, a "forward" simulator calculates power flows in the same direction as they are in an actual vehicle. Therefore, it is a better representation in the sense of truthfulness. In addition, the "forward" model is able to integrate dynamics [16] and clearly we have to use this for our research. The main drawback it brings is slower simulation speed.

2. OBJECTIVE METRICS FOR FUEL ECONOMY, PERFORMANCE AND DRIVEABILITY

The fundamental requirements for simulation implementable measures of fuel economy, performance and driveability are objective and quantitative. Unlike fuel economy and performance, driveability describes vehicle responsiveness, operating smoothness and driving comfort, and is difficult to be expressed objectively. Conventional

scorecard type evaluation is time consuming and expensive since it can only be done by a human driver after a physical vehicle is available. More importantly, it is subjective and not repeatable, even when rated by the same evaluator. This paper summarizes some objective driveability metrics that can be revealed in our low-frequency dynamic model. Evaluating maneuverability, stability, noise level and harshness etc. is not the goal here.

2.1 Fuel Economy Metrics

Fuel economy is defined as volumetric fuel consumption per distance traveled in the unit of *mpg*. Sovran and Blaser stated comprehensive insights on fuel economy in [17] and also investigated various ways to improve it. Utilizing hybrid drivetrain, CVT or ISA can improve fuel economy by 7~12%, 6~11% and 6~12% respectively, from a baseline vehicle.

In simulations, automotive engineers usually estimate city and highway fuel economy on predefined driving cycles. Federal Urban Driving Schedule (FUDS) and Federal Highway Driving Schedule (FHDS) are the two most commonly used cycles. There also exist numerous other standard and customer defined driving cycles, e.g. New York City Cycle (NYCC), New European Driving Cycle (NEDC), Japan 10/15/1015, military driving cycles, etc.

2.2 Performance Metrics

Vehicle performance includes acceleration time, top speed, stopping distance, gradeability and towing capability.

0 to 60 *mph* acceleration test is widely used to evaluate vehicle acceleration capability. It appears in almost every simulation tool which contains an acceleration test. 30~50 *mph* acceleration is used to approximate vehicle merging to highway and 50~70 *mph* acceleration simulates a passing event on highway.

Top speed is the maximum speed a vehicle can reach. For an HEV, it implies that the electric machine can only help in the first portion of the acceleration, but cannot assist during the whole acceleration from zero speed to top speed, if it is defined as the sustainable maximum vehicle speed.

Whether a vehicle can stop in time is an important criterion for safety. Stopping distance is the vehicle displacement from the time when a driver makes the decision to slow down to the time when the vehicle is fully stopped.

In the gradeability test, we need to check the maximum slope a vehicle can maintain at a predetermined constant speed, e.g. 55 *mph*.

Towing capability is how much a vehicle can tow when it is operating under the same test conditions as for non-towing cases. It includes all driving scenarios we just mentioned.

2.3 Driveability Metrics

2.3.1 Vibration Dose Value (VDV). Vibration dose value is a mathematical concept which describes the total vibration dose received by being in contact with a vibrating surface over a specific period of time, taking account of the direction of the vibration, frequency characteristics and time history [18]. The VDV is more sensitive to peaks than the RMS introduced below and hence is a better indicator of rides that contain shocks, jolts and jars [19]. The expression for the VDV is as follows:

$$VDV = \left(\int_{t_0}^{t_f} \tilde{a}^4(t)dt \right)^{\frac{1}{4}} \tag{1}$$

The variable $\tilde{a}$ in Eq. (1) [20] is the vehicle acceleration filtered by a band-pass filter with bandwidth of 1 to 32 *Hz*. t_0 is the starting time and t_f is the final time.

2.3.2 Acceleration Root Mean Square (RMS) Value. Acceleration RMS value calculates the average vehicle acceleration:

$$RMS = \sqrt{\int_{t_0}^{t_f} \tilde{a}^2 dt / \left(t_f - t_0\right)} \tag{2}$$

2.3.3 Acceleration/Deceleration Jerk. Jerk is the first derivative of vehicle acceleration. The magnitude of jerk is highly correlated with driving comfort and safety. According to [19, 21], an acceptable jerk is 2 m/s^3 and a comfortable jerk is 1 m/s^3.

2.3.4 Maximum Transient Vibration Value (MTVV) / Maximum G-force. MVTT provides information on shock loads which are not revealed in the acceleration RMS value. Maximum G-force is the ratio of the maximum amplitude of acceleration or deceleration over the gravity acceleration in the unit of *g*.

2.3.5 Tip-in/Tip-out Response. Besides the amplitude of acceleration, the shape of the acceleration profile is also critical to ride comfort. Figure 2 is an undesirable tip-in response at wide open throttle [22]. Apparently, delay and sag in the acceleration should be minimized and oscillations need to be suppressed.

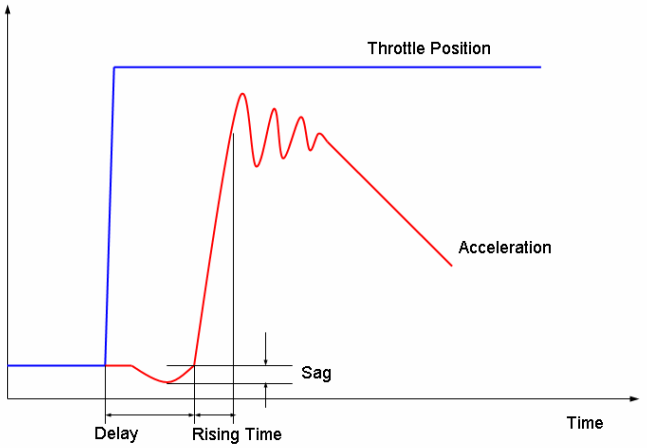

Figure 2. Tip-in response

3. MODEL DESCRIPTION

3.1 Engine

A 2.2 liter 4-cylinder SI engine is selected for this HEV. It has maximum torque of 209 *N.m* at 3000 *rpm* and maximum power of 119 *kw* around 6000 *rpm*. We assume exhaust gas recirculation (EGR) is realized internally by variable valve timing (VVT) and spark

advance (SA) remains constant in certain operating conditions (hard acceleration/deceleration and other driving conditions). A time domain mean-value engine model is broken down into four subsystems: electronically controlled throttle body, intake manifold, combustion and crank shaft.

3.1.1 Electronically Controlled Throttle Body (ETB). Unlike a conventional mechanically driven throttle which has a fixed relation between accelerator pedal position and throttle valve position, an electronically controlled throttle body (ETB) has these two positions decoupled with programmable control. The ETB contains a DC motor with reduction gears and return-springs [23]. Electronic throttle control (ETC) initially found its applications in traction control and cruise control. Recent research shows that it is also useful in reducing torque oscillations and emissions, which in turn provides good fuel economy and driveability [24].

Wit, Kolmanovsky and Sun have created a second order nonlinear electronic throttle model by applying dynamic LuGre model for friction torque [22]. This model is rather complicated for our purpose. Therefore, the ETB is identified as a first order system, i.e. the output air mass flow rate follows the requested input with a lag:

$$\tau_{etb}\frac{d\dot{m}_{th}}{dt} = -\dot{m}_{th} + \dot{m}_{th\_req} \tag{3}$$

The actual mass flow rate of air entering the intake manifold decreases with lower throttle and higher manifold pressure. This is considered by setting a limit, which is apparently a function of throttle and manifold pressure (see Fig. 3) represented by:

$$\dot{m}_{th} \le \dot{m}_{th\_limit} \tag{4}$$

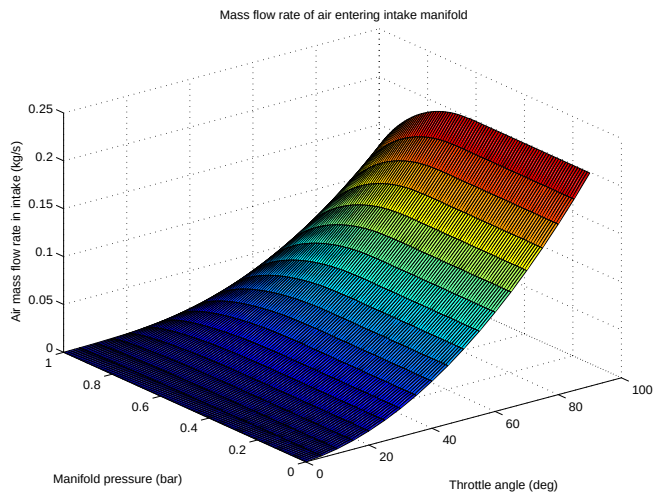

Figure 3. Effect of manifold pressure on intake air mass flow rate

3.1.2 Intake Manifold. The intake manifold is the plenum between the ETB and the engine cylinders. Equation (5) describes a mean-value filling-and-emptying intake model based on the continuity principle and the ideal gas law [25]. The total air that goes into the cylinders is expressed in an empirical Eq. (6).

We assume engine air fuel ratio (AFR) is always well maintained at stoichiometric operating conditions, so fuel dynamics are not modeled here. Fuel consumption is thus calculated as the total air mass flow rate entering the cylinders divided by 14.7.

$$\frac{dp_m}{dt} + \frac{R_m T_m}{V_m}\dot{m}_{cyl} = \dot{m}_{th}\frac{R_m T_m}{V_m} \tag{5}$$

$$\dot{m}_{cyl} = M_1\omega_e + M_2 p_m + M_3\omega_e p_m + M_4\omega_e p_m^2 \tag{6}$$

3.1.3 Combustion. Engine combustion takes air and fuel as inputs and produces torque and exhausts with losses. Torque production from combustion is usually estimated by a regression model that takes air flow, SA, AFR and engine speed into account. Since AFR is assumed to be constant in this model, its effect on produced torque is combined into T_0 term. The engine torque therefore becomes

$$T_e = T_0 + T_1\dot{m}_{cyl}(t - t_d)/\omega_e + T_2 SA + T_3 SA^2 + T_4\omega_e + T_5 SA\omega_e + T_6\omega_e^2 \tag{7}$$

T_e in Eq. (7) is the net engine torque which considers both engine nominal production and friction torques. Air in this equation is delayed by t_d which varies in the time domain due to varying engine speed. The engine torque is bounded by wide open throttle and minimum throttle torques according to

$$t_d = \frac{2\pi}{\omega_e} \tag{8}$$

$$T_{e\_\min} \le T_e \le T_{e\_\max} \tag{9}$$

3.1.4 Crank Shaft. Crank shaft speed dynamics are intrinsically based on Newton's second law for a rotational object. The ISA torque is added into the ICE torque as the total traction torque on the engine side. T_p in Eq. (10) represents the load torque from the torque converter pump. Idle and redline are the physical speed constraints for the engine. These relationships are represented as

$$J_1\frac{d\omega_e}{dt} = T_e + T_{isa} - T_p - B_{eng}\omega_e \tag{10}$$

$$idle \le \omega_e \le redline \tag{11}$$

3.2 Integrated Starter/Alternator (ISA)

In this research, we use a 30 *kw* (peak) induction machine as the ISA due to its wide torque-speed range, high performance, ruggedness, better failure mode and low cost [26]. This ISA is connected directly to the engine to replace the flywheel. Its main functions include starting the engine, power assistance, regenerative braking and compensating torque fluctuations.

For simplicity, models of an ISA, power electronics and a battery pack are lumped together as one single model. Battery state of

charge (SOC) is then estimated through power integration instead of current integration. Equations (12-17) characterize the ISA/battery dynamics and their physical limitations:

$$\tau_{isa}\frac{dT_{isa}}{dt} = -T_{isa} + T_{isa\_req} \tag{12}$$

$$\frac{d(SOC)}{dt} = -\frac{T_{isa}\cdot\omega_{isa}}{K_{SOC}\cdot\eta} \tag{13}$$

$$T_{isa\_\min} \le T_{isa} \le T_{isa\_\max} \tag{14}$$

$$\omega_{isa\_\min} \le \omega_{isa} \le \omega_{isa\_\max} \tag{15}$$

$$SOC_{\min} \le SOC \le SOC_{\max} \tag{16}$$

$$P_{recharging} \le \frac{P_{out}}{\eta} \le P_{discharging} \tag{17}$$

3.3 Torque Converter (TC)

Torque converters (TCs) act as hydraulic dampers to interrupt vibration propagation originated from either engines or road bumps and to provide torque multiplication during vehicle launch [7]. Since the TC is essentially a damper, losses are not negligible. However, these losses can be reduced by employing a TC bypass clutch, which mechanically connects the TC pump and the turbine when the clutch is engaged. This connection improves TC efficiency at the price of losing the capability to absorb oscillations in the drivetrain. A compromising solution is proposed by Hiramatsu et al., allowing 1 to 2 % of clutch slip to achieve similar results as the TC is working as a damper [27]. Obviously, we desire to minimize this slip for efficiency consideration. This type of bypass clutch is a so-called minimal slip-type TC clutch.

The torque converter is expressed with a regression model based on Kotwicki's research of more than twenty years ago [9]. In this model, there are three modes in the forward drive case (power is flowing from the engine to the wheels) and two modes in the backward drive case (overrun case), shown in Eqs. (18-23).

This TC has the maximum torque ratio (turbine torque over pump torque) of about 1.65 and the coupling point at speed ratio (turbine speed over pump speed) of 0.88. Its efficiency before the coupling point is lower than 90% and that in the lockup mode is around 99%.

FORWARD: ($\omega_p > \omega_t$)
Torque multiplication mode: ($T_t > T_p$)

$$T_p = b_1\omega_p^2 + b_2\omega_p\omega_t + b_3\omega_t^2 \tag{18}$$

$$T_t = c_1\omega_p^2 + c_2\omega_p\omega_t + c_3\omega_t^2 \tag{19}$$

Torque coupling mode: ($T_t = T_p$)

$$T_p = T_t = a_1\omega_p^2 + a_2\omega_p\omega_t + a_3\omega_t^2 \tag{20}$$

Lockup mode:

$$\omega_p \approx \omega_t \tag{21}$$

$$T_p = T_t \le T_{clutch\_\max} \tag{22}$$

BACKWARD (overrun): ($\omega_t > \omega_p$)
Torque coupling mode: ($T_t = T_p$)

$$T_t = T_p = d_1\omega_p^2 + d_2\omega_p\omega_t + d_3\omega_t^2 \tag{23}$$

Lockup mode: the same as in the forward drive case.

3.4 Continuously Variable Transmission (CVT)

Compared to a drivetrain equipped with a stepped-gear transmission, the one with a CVT has better overall efficiency and driveability. A variable pulley type CVT with a metal V belt is used here. The CVT ratio is controlled by changing the radii of the primary and the secondary pulleys with a hydraulic control system and it behaves close to a first order system. The following equations summarized the CVT model:

$$r_{cvt} = \frac{\omega_{cvt\_s}}{\omega_{cvt\_p}} \tag{24}$$

$$T_{cvt\_s} = \frac{T_{cvt\_p}}{r_{cvt}}\eta_{cvt} \tag{25}$$

$$\tau_{cvt}\frac{dr_{cvt}}{dt} + r_{cvt} = r_{cvt\_req} \tag{26}$$

$$J_2\frac{d\omega_t}{dt} = T_t - T_{cvt\_p} \tag{27}$$

$$J_3\frac{d\omega_{cvt\_s}}{dt} = T_{cvt\_s} - T_{fd} \tag{28}$$

$$r_{cvt_{\min}} \le r_{cvt} \le r_{cvt_{\max}} \tag{29}$$

3.5 Final Drive (FD)

A final drive is represented as a gear set. The ratio is defined as the final drive speed over the driveshaft speed. Efficiency of the final drive is simplified by taking a constant value:

$$r_{fd} = \frac{\omega_{fd}}{\omega_{ds}} \tag{30}$$

$$T_{ds} = T_{fd}r_{fd}\eta_{fd} \tag{31}$$

3.6 Driveshaft

Shaft flexibility is modeled as lumped compliance, which is helpful in absorbing oscillations in the drivetrain. The nonlinear damper is characterized as a function of driveshaft speed and its square:

$$\frac{dT_{wh}}{dt} = K_{ds}\left(\omega_{ds} - \omega_{wh}\right) \tag{32}$$

$$T_{fd} = T_{wh} + D_1\omega_{ds} + D_2\omega_{ds}^{\ 2} \tag{33}$$

3.7 Brake-By-Wire (BBW)

Brake-by-wire (BBW) systems were initially designed for aircrafts and now are in Mercedes-Benz SL500 cars on the market [28]. In a vehicle incorporating a BBW, a driver's braking intention is

transmitted electronically from the brake pedal to electro-hydraulic or electro-mechanic brake actuators located at each wheel [28]. Simple structure and cheap realization with easy adaptation to other systems like anti-lock brake system (ABS) via software will enable BBWs to be utilized into more and more mass production vehicles.

Equation (34) describes the first order behavior of a BBW driven by a motor:

$$\tau_{brk}\frac{dT_{brk}}{dt} = -T_{brk} + T_{brk\_req} \tag{34}$$

$$F_{tr} = \frac{T_{wh} - T_{brk}}{R_{wh}} \tag{35}$$

3.8 Vehicle

Vehicle dynamics are captured with Newton's second law for a longitudinal moving object. Resistance forces including aerodynamic, rolling resistance and gravity forces are expressed as follows:

$$M \cdot \frac{dV}{dt} = F_{tr} - F_a - F_r - F_g \tag{36}$$

$$F_a = \frac{1}{2}\rho_{air} C_d A_f V^2 \tag{37}$$

$$F_r = MgC_r \cos(grade) \tag{38}$$

$$F_g = Mg \sin(grade) \tag{39}$$

3.9 Controller

A simple control strategy containing five states, i.e. stop, start, hard acceleration, hard deceleration and cruise, is used here. This controller sends out air mass flow rate, ISA torque, brake torque, engine ON/OFF, TC lockup and CVT ratio requests according to pedal position, vehicle velocity and battery state of charge (SOC). More sophisticated control policies will be developed to optimize contradictory criteria of fuel economy, performance and driveability in the near future.

3.10 Driver

A "Forward" simulator needs a "Driver" block to imitate a human driver generating accelerator and brake pedal commands. This is accomplished by feeding vehicle speed difference between the desired and the actual into a PID controller [15].

4. SIMULATION

4.1 Simulator

The dynamic model described in the last section is implemented in MATLAB®/SIMULINK®. All the components are programmed as subsystems in a library. In practice, the simulation sampling frequency needs to be about 5 to 10 times of the highest frequency in the system. Parameters of this vehicle are selected from various resources [30-34].

Besides the driving cycles mentioned in section 2.1, four extra maneuvers are included in the simulator to evaluate vehicle performance. They are the 0 to top speed then back to 0 *mph* hard acceleration/deceleration test, the 30~50 *mph* and the 50~70 *mph* passing maneuvers, and the gradeability test maneuver. The hard acceleration/ deceleration test is able to evaluate 0~60 *mph* acceleration, top speed and stopping distance. This maneuver is designed as two steep ramps close to step functions at the initial time and 100 *s*, so that the 'Driver' will interpret these two ramp speed commands as full accelerator and brake pedal requests respectively. In the 30~50 *mph* acceleration test, the vehicle should reach steady state velocity before it starts to accelerate from 30 *mph*. A moderate ramp from 0 to 30 *mph* will lead the vehicle to reach 30 *mph* and it will stabilize at this speed during a 10 second constant speed request period. Then, the vehicle will speed up to track the 30~50 *mph* steep ramp command. The 50 to 70 *mph* maneuver is implemented in a similar way.

4.2 Simulation Results

The following results are for the hard acceleration/ deceleration test (see Fig. 4). In order to reveal powertrain excitation dynamics and to estimate the sustainable vehicle top speed, the ISA was shut down abruptly when the vehicle reached a quarter *mile*. The CVT ratio is set to maintain constant maximum power from the engine during acceleration.

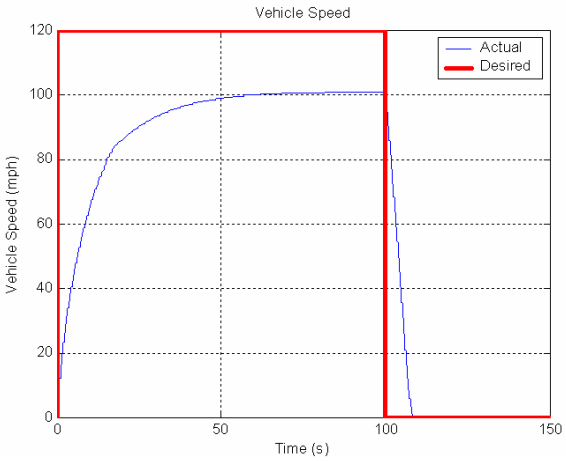

Figure 4. Actual vehicle velocity in acceleration/ deceleration test

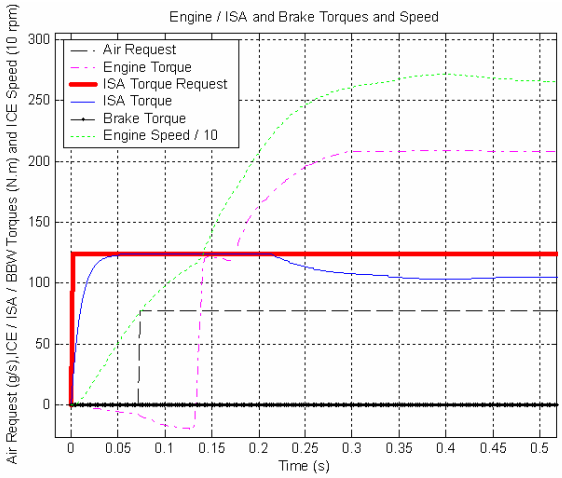

Figure 5. Vehicle behaviors during launch

0 to 60 *mph* acceleration, top speed and top speed to 0 mph stopping distance of this vehicle are 8.71 *s*, 101 *mph* and 172.8 *m* as indicated in Fig. 4. Figure 5 depicts ISA and BBW torque commands, engine air request and speed. It takes the ISA approximately 70 *ms* to start the engine, while the engine torque remains negative for another 60 *ms* after it is started due to the ETB lag and the torque production delay. Actual ISA torque follows the torque request as a first order system and begins to drop when it enters the constant-power operating region after 200 *ms*.

Figures 6 and 7 describe TC and CVT behaviors. At the very beginning and around 17 *s* of the test, we observe oscillations of less than 5 *Hz* in torques and speeds. These are caused by sudden introduction and removal of the ISA torque.

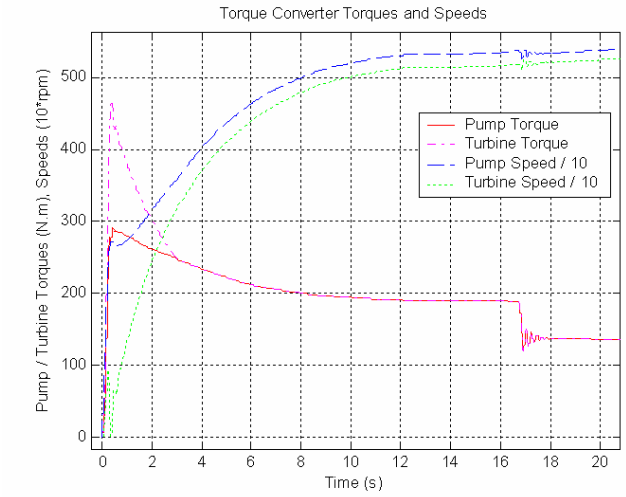

Figure 6. TC pump/turbine torques and speeds

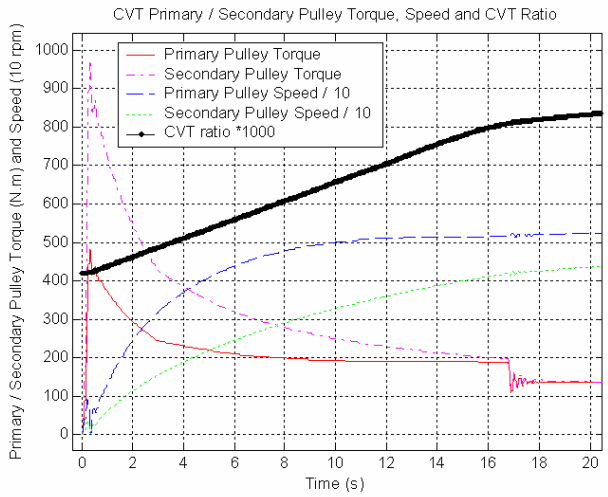

Figure 7. CVT torques, speeds and ratio

Acceleration for the first five seconds depicted in Fig. 8 shows both delay and oscillations. Apparently, these oscillations are propagated from the upstream. Hard deceleration starting at 100 *s* causes similar vibrations in the drivetrain. Ultimately, all of these vibrations should be minimized in the control strategy. The maximum acceleration/deceleration is about 0.8/0.65 *g*, which in turn results in high jerk of more than 50 m/s^3 for less than 50 *ms*. The VDV and the RMS values of this maneuver are 1.97 $m/s^{1.75}$ (7.33 $m/s^{1.75}$ if normalized to 8 hours) and 1.58 m/s^2, which indicate acceptable overall dosage.

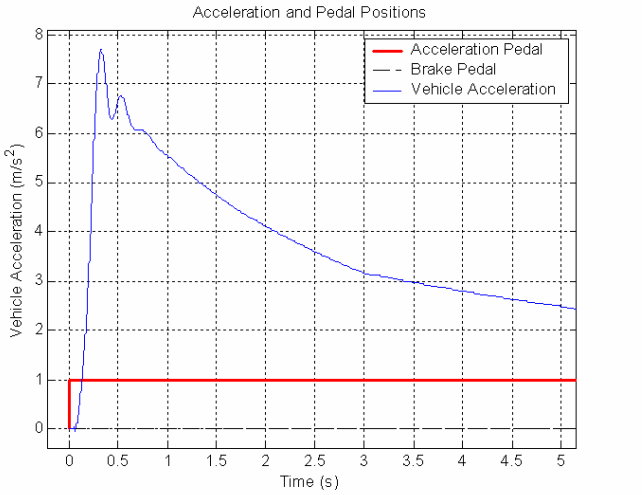

Figure 8. Vehicle acceleration profile

Estimated city (FUDS) and highway (FHDS) mileage of this vehicle is about 21.7 and 25 *mpg* respectively. Fuel economy could be improved with controller targeting to minimize fuel consumption.

5. CONCLUSIONS AND FUTURE WORK

The low-frequency nonlinear dynamic model in this paper is effective in describing powertrain dynamics, estimating fuel economy, predicting vehicle performance, and evaluating driveability with adequate fidelity. This ten-state, six-input (four numerical and two logical) model and the simulator provide a software test bed for powertrain dynamics analysis and control strategy testing. It allows the designers to exploit tradeoffs between energy storage and conversion systems to achieve optimization in the face of multiple conflicting criteria of fuel economy, performance and driveability.

Our future work will concentrate on model validation using a prototype (such as Future Truck) or the hardware-in-the-loop (HIL) lab [35] as well as optimal control algorithm development, implementation and validation.

REFERENCES

[1] Grava S., 2003, *Urban Transportation Systems Choices for Communities*, McGraw-Hill, New York.

[2] Soong W., Ertugrul N., Lovelace E., Jahns T., 2001, "Investigation of Interior Permanent Magnet Offset-Coupled Automotive Integrated Starter/Alternator", *Proceedings of Industry Applications Conference*, **1**, pp. 429-436.

[3] Frijlink P., Schaerlaeckens W., Tillaart.E., Haas J., 2001, "Simulation of a Vehicle with an ICE, CVT, and ISG Powertrain – A Pre-study for Concept Evaluation and Dimensioning", *SAE paper 2001-01-3453*.

[4] Miyano T., Hubbard M., 1990, "Internal Combustion Engine Intake-Manifold Aspiration Dynamics", *Journal of Dynamic Systems, Measurements, and Control*, **112**, pp. 596-603.

[5] Sung N., Song J., Jeong Y., Kim C., 1996, "Flow Modeling for the Branched Intake Manifold Engine", *SAE paper 960079*.

[6] Krause P., Wasynczuk O., 1989, *Electromechanical Motion Devices*, McGraw-Hill, New York.

[7] Hrovat D., Tobler W., 1985, "Bond Graph Modeling and Computer Simulation of Automotive Torque Converters", *Journal of Franklin Institute*, **319**, pp. 93-114.

[8] Pfiffner R., 2001, "Optimal Operation of CT-Based Powertrains", *Ph.D. Dissertation, Swiss Federal Institute of technology*, Zurich, Switzerland.

[9] Kotwicki A., 1982, "Dynamic Models for Torque Converter Equipped Vehicles", *SAE paper 820393*, pp. 103-117.

[10] Yurkovich S., Simpson M., 1997, "Comparative Analysis for Idle Speed Control: A Crank-Angle Domain Viewpoint", *Proceedings of American Control Conference, Albuquerque, NM*, pp. 178-283.

[11] Butts K., Sivashankar N., Sun J., 1999, "Applications of l_1 Optimal Control to the Engine Idle Speed Control Problem", *IEEE Transactions on Automatic Control*, **34**, pp. 386-396.

[12] Sun P., Powell B., Hrovat D., 2000, "Optimal Idle Speed Control of an Automotive Engine", *Proceedings of American Control Conference, Chicago, IL*, pp. 1018-1026.

[13] Fekete N., Nester U., Gruden I., Powell J., 1995, "Model-Based Air-Fuel Ratio Control of a Lean Multi-Cylinder Engine", *SAE paper 950846*, pp. 71-83.

[14] Liu S., Stefanopoulou A., 2002, "Effects of Control Structure on Performance for an Automotive Powertrain with a Continuous Variable Transmission", *IEEE Transactions on Control Systems Technology*, **10**, pp. 701-708.

[15] Rizzoni G., Guezennec Y., Brahma A., Wei X., Miller T., 2000, "VP-SIM: A Unified Approach to Energy and Power Flow Modeling Simulation and Analysis of Hybrid Vehicles", *Proceedings of the 2000 Future Car Congress*, *Arlington, Virginia*.

[16] Wipke K., Cuddy M., Burch S., 1999, "ADVISOR 2.1: A User-Friendly Advanced Powertrain Simulation Using a Combined Backward/Forward Approach", *IEEE Transactions on Vehicular Technology*, **48**, pp. 1751-1761.

[17] Sovran G., Blaser D., "A Contribution to Understanding Automotive Fuel Economy and Its Limits", *SAE paper 2003-01-2070*.

[18] turva.me.tut.fi/iloagri/fore/vib2.htm

[19] www.atsb.gov.au/road/rpts/cr203/std_vib.cfm

[20] Megli T., Haghgooie M., Colvin D., 1999, "Shift Characteristics of a 4-Speed Automatic Transmission", *SAE paper 1999-01-1060*.

[21] Chen Y., 1995, "Effect of Communication Delays on the Performance of Vehicle Platoons", *M.S. Dissertation, University of California, Berkeley*, Berkeley, CA.

[22] Wicke V., Brace C., Vaughan N., 2000, "The potential for Simulation of Driveability of CVT Vehicles", *SAE paper 2000-01-0830*.

[23] Wit C., Kolmanovsky I., Sun J., 2001, "Adaptive Pulse Control of Electronic Throttle", *Proceedings of American Control Conference, Arlington, VA*, pp. 2872-2877.

[24] Streib H., Bischof H., 1996, "Electronic Throttle Control (ETC): A Cost Effective System for Improved Emissions, Fuel Economy, and Driveability", *SAE paper 960338*, pp. 169-176.

[25] Rizzoni G., 2000, "Powertrain Dynamics", *Class Notes for ME 781 at the Ohio State University, Columbus, OH*.

[26] Kahlon G., Mohan R., Liu N., Rehman H., 1999, "A Case Study of Starting Power Requirement for Visteon Integrated Starter-Alternator System", *Proceedings of Digital Avionics Systems Conference*, **2**, pp. 8.B.4-1 – 8.B.4-7.

[27] Hiramatsu T., Akagi T., Yoneda H., 1985, "Control Technology of Minimal Slip-Type Torque Converter Clutch", *SAE paper 850460*, pp. 127-135.

[28] Ross P., 2003, "Top 10 Techno-Cool Cars", *IEEE Spectrum*, pp. 30-35.

[29] Aidemark J., Vinter J., Folkesson P., Karlsson J., 2002, "Experimental Evaluation of Time-Redundant Execution for a Brake-by-Wire Applications", *IEEE Proceedings of the International Conference on Dependable Systems and Networks*.

[30] www.bgsoflex.com/airdragchart.html

[31] www.teknett.com/pwp/drmayf/dragcd~1.hrm

[32] www.school-for-champions.com/science/frictionrolling2.htm

[33] www.toyota.com/html/shop/vehicles/prius/spec/prius_specs.html

[34] www.oldsmobile.com/alero/features/specifications.htm

[35] Powell B., Sureshbabu N., Bailey K., Dunn M., 1998, "Hardware-In-The-Loop Vehicle and Powertrain Analysis and Control Design Issues", *Proceedings of American Control Conference, Philadephia, PA*, pp. 483-492.